Molecular Crystals and Liquid Crystals
Publication details, including instructions for authors and subscription information:
http://www.tandfonline.com/loi/gmcl20

Dynamics of a Light Driven Molecular Motor

P. Palffy-Muhoray [a], T. Kosa [a] & E. Weinan [b]

[a] Liquid Crystal Institute, Kent State University, Kent, OH, 44242

[b] Mathematics Department, Princeton University, Princeton, NJ, 08544

Version of record first published: 18 Oct 2010

To cite this article: P. Palffy-Muhoray, T. Kosa & E. Weinan (2002): Dynamics of a Light Driven Molecular Motor, Molecular Crystals and Liquid Crystals, 375:1, 577-591

To link to this article: http://dx.doi.org/10.1080/10587250210584

Mol. Cryst. Liq. Cryst., Vol. 375, pp. 577-591

1058-725X/02 $12.00 + .00

Dynamics of a Light Driven Molecular Motor

P. PALFFY-MUHORAY[a], T. KOSA[a] and E. WEINAN[b]

[a]*Liquid Crystal Institute, Kent State University, Kent, OH 44242 and*
[b]*Mathematics Department, Princeton University, Princeton, NJ 08544*

Molecular motors play key roles in areas ranging from biological transport to emerging nanotechnology. They produce current as a result of transfer of energy but not of momentum from a source; many molecular motor scenarios are based on the translational Brownian ratchet mechanism. Here we consider the mechanism of photoalignment of liquid crystals by a photosensitive alignment layer. We show that the photoalignment is due to an orientational ratchet mechanism, where the azo-dye molecules, functionalized into a polymer alignment layer, when irradiated by polarized light act as the rotors of Brownian motors which reorient the bulk liquid crystal against an elastic restoring torque. Results of this photoalignment experiment can be obtained directly from a remote experiment set up at the Liquid Crystal Institute, via the WWW. In addition to experimental results, we present a detailed Fokker-Planck description of this system. We discuss the implementation and the results of numerical simulations, and compare these with the experimentally observed dynamics.

INTRODUCTION

It is well known that light can exert a force on matter; radiation pressure on a reflecting metal surface, or a black absorbing surface are well known examples. It is perhaps less well known that light falling from vacuum on a dielectric interface exerts a force which attracts the interface towards the source of light[1]. In 1936, R.A. Beth showed that light can also exert a torque[2]; in his example, the torque, along the wave vector of light, was due to the transfer of intrinsic (spin) angular momentum from the radiation field to the material. In 1969, A. Saupe showed that light can also exert a torque, perpendicular to the wave vector, on liquid crystals[3]; this effect has subsequently been rediscovered by others[4,5,6,7], and has been the subject of considerable attention. In Saupe's experiment, the torque is due to the transfer of extrinsic (orbital) angular momentum from the radiation field to the material[8].

In 1990, Janossy showed that by adding a small amount of dichroic dye to the liquid crystal, the threshold intensity for the light induced reorientation is reduced by some two orders of magnitude[9,10]. Since in this case the transfer of extrinsic

angular momentum from light is also reduced by some two orders of magnitude while the elastic restoring torques remain unaltered, it is clear that the torque felt by the liquid crystal cannot originate in angular momentum transfer. Understanding the details of angular momentum balance in this system posed an interesting and challenging problem. Aspects of angular momentum transfer and molecular friction have been discussed by Marrucci et al[11]. We have suggested that the observed 'rotation without torque' is an orientational version of the translational ratchet mechanism, capable of producing 'motion without force', proposed by Astumian[12] and Prost[13], and that the torque, originating at the cell walls, is carried by viscous shear to the dye molecules, which act as rotors of a Brownian motor[8]. Subsequently, this model has been significantly expanded[14,15].

In this paper, we argue that photoalignment by dye doped photosensitive alignment layers can also be due to the ratchet mechanism, where the dichroic dye molecules in the alignment layer act as rotors of Brownian motors.

BIOLOGICAL TRANSPORT

It is interesting to explore parallels in the understanding of angular momentum balance in the photoalignment of liquid crystals, and of the mechanism of transport in biological systems. Essentially all living organisms (the eukaryotic cells of yeasts, plants, animals) contain 'motor proteins'. Two well known examples are kinesins and myosins. Kinesin has two active heads, it hydrolyzes ATP, and moves along processively along microtubules.

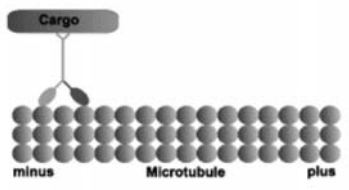

FIGURE 1. Schematic of kinesin carrying cargo along a microtubule.

Myosin also has two active heads, it also hydrolyzes ATP, and it moves processively along actin fibers. Although myosin is involved in a great variety of cell functions, it is perhaps its best known for its role is in muscle tissue. The actin fibers in muscle are connected to Z-membranes forming the end of sarcomeres; the motion of the myosin heads on the actin fibers results in tension of the myosin strands, contraction of the sarcomeres, and of the muscle fiber[16]. The myosin fibers are approximately 1.55μm long, exert a force of $\sim 5pN$ per attached head, the step-size is $5.5nm$ and there is one step/ATP-ase reaction.

The mechanisms responsible for the transport of both kinesin and actin has been the subject of considerable discussion in the literature. The conventional view has been that myosin transport takes place via a 'lever-arm swinging' model, while actin transport takes place via 'hand-over-hand' motion[17].

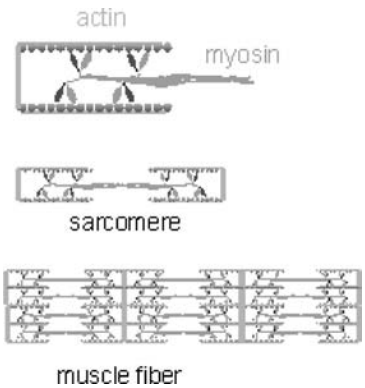

FIGURE 2. Schematic of myosin movement resultsing in muscle contraction.

Recent experimental results have however cast doubt on the validity of these models. Ishii and Yanagida showed[18] that processive transport can be observed in myosin subfragments which are without the full mechanical 'lever-arm' component, indicating that the 'lever-arm' model cannot adequately explain the mechanism of the observed motion. Similarly, Okada and Hirokawa developed a mutant superfamily of one-headed kinesin, also capable of processive transport[19]. Their result suggested that the 'hand-over-hand' motion cannot adequately explain the *mechanism of the observed motion. The conventional mechanical models thus apparently failed to explain the details of the observed processive transport.
It has now been proposed that both in the case of actin and of myosin, the mechanism for the observed 'motion without force' is the biased Brownian ratchet[20,21]; that is, essentially the same mechanism which is responsible for the anomalous threshold reduction in the Janossy effect, and, as we argue below, for photoalignment by dyed photosensitive alignment layers.

MOTORS AND DIFFUSIVE TRANSPORT

In view of considerable recent discussion of molecular motors in the literature, it is interesting to inquire into the definition of a motor. We note that even conventional motors have the feature that they give rise to 'motion without force'. For example, in the road-car system, the car typically moves, not as a results of an externally applied force, but because the motor of the car causes one part of the system (the road) to exert a force on the other (the car) without any momentum transfer from outside the system. A working definition of motor may therefore be: *that wich*

causes motion in a system without momentum transfer from the outside, or, alternately, *a machine that uses energy but not momentum to drive a current.*

Diffusive transport is the name given to model processes[22] which can drive a current of particles against an opposing viscous force. Unlike in conventional motors, intertia does not play a role. One early example of diffusive transport is the beautiful model proposed by R. Landauer[23], which has become known as Landauer's Blowtorch. Here particles experience a spatially periodic symmetric sinusoidal potential as well as a periodic temperature field, as shown in Fig. 3.

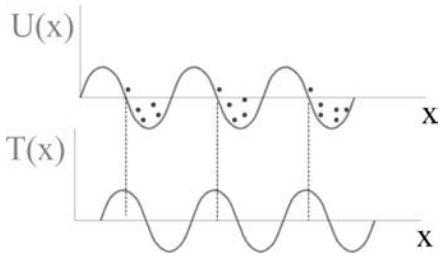

FIGURE 3. Landauer's Blowtorch. Particles experience a static sinusoidal potential as well as a sinusoidal temperature field; the temperature is shifted $\lambda/4$ relative to the potential.

Since the temperature is shifted relative to the potential, particles near the left side of the valleys are at a higher temperature than those near the right; consequently they are more likely to be thermally excited over the potential barrier and diffuse to the left. The heat source in this arrangement therefore drives a steady current of particles against an opposing viscous force; the current flows without momentum transfer from the outside.

A schematic of the translational ratchet of Astumian[12] and Prost[13] is shown in Fig. 4.

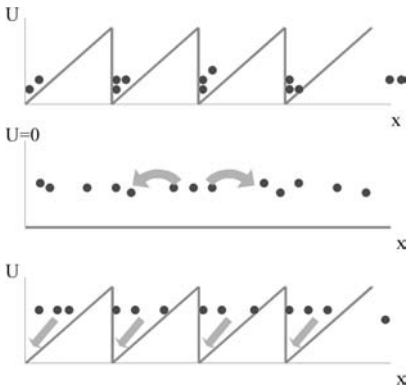

FIGURE 4. Schematic of the translational ratchet.

When the asymmetric potential U is turned OFF, particles diffuse evenly in both left and right directions, and the net current is zero. When the potential is turned ON, the particles undergo directed diffusion under the influence of the potential, resulting in a net current to the left. A salient feature of the ratchet is a spatially periodic asymmetric potential which is periodic in time. The process is diffusive rather than intertial; the potential drives a current against an opposing viscous force. Turning the potential ON and OFF requires a transfer of energy, but not of momentum.

We now consider a photoinduced twist experiment, and argue that the process underlying the photoalignment is an orientational ratchet mechanism.

PHOTOINDUCED TWIST EXPERIMENT

The sample cells used in the experiment consist of two glass plates, separated by $20\mu m$ spacers, and containing the liquid crystal 5CB between the plates. One plate was coated with a mechanically buffed polyimide layer which is expected to give strong planar anchoring. The other plate was coated with a 300 Å thick photosensitive layer of PMMA into which the azo-dye Disperse Red I has been functionalized. The chemical structure of the photosensitive alignment layer is shown in Fig. 5.

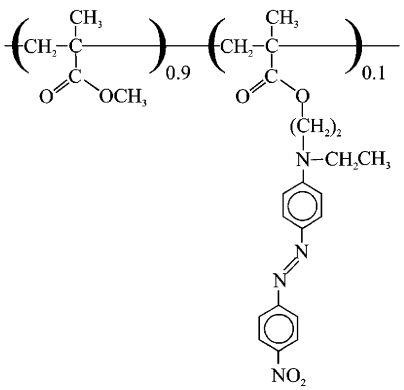

FIGURE 5. Chemical structure of the PMMA layer with the functionalized DR I dye.

A schematic of the photoinduced twist experiment is show in Fig. 6. If there is no light incident on the photosensitive alignment layer, the alignment of the director in the cell is everywhere planar, as dictated by the strong anchoring by the

mechanically buffed polyimide layer. When the cell is irradiated by plane polarized light at $\lambda = 514nm$ and at $20mW$ of power from a CW Ar+ laser, with polarization parallel to the director, a twist deformation develops in the cell as shown in Fig. 6.

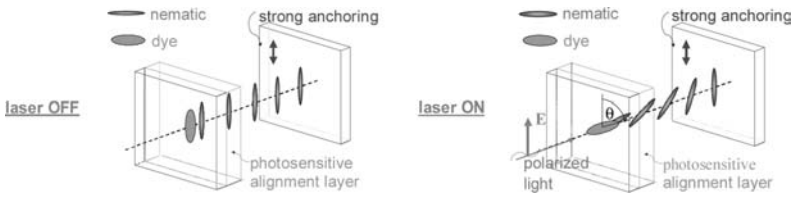

FIGURE 6. Schematic of the photoinduced twist experiment

To measure the twist, a pump-probe arrangement was implemented; a He-Ne laser illuminating the sample between crossed polarizers was used as the probe. The experimental setup is shown in Fig. 7.

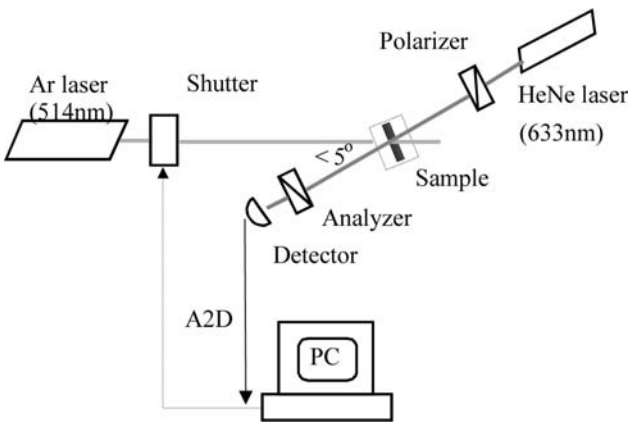

FIGURE 7. Schematic of the experimental setup.

When the cell is in the uniform planar state, the detector receives no signal, since the polarizer and analyzer are crossed. As the photoinduced twist develops under the influence of the pump beam, the transmitted intensity increases; the transmitted intensity thus gives a measure of the twist in the cell.

REMOTE EXPERIMENT ON THE WEB

In order to give interested investigators the opportunity to carry out this experiment, equipment has been set up at th Liquid Crystal Institute at Kent State University which allow this experiment to be carried out remotely, via the World Wide Web. Any user with Internet access and a Web browser can access the experiment at http://experiment.lci.kent.edu. In addition to obtaining access to background material describing the experiment and the equipment, remote users can control, in real time, the shutter, the pump polarization and the pump intensity. They can also obtain the signal from the detector as well as real video images of the experiment. A typical frame, showing the user interface, detector signal as function of time and video frame of the equipment is shown in Fig. 8.

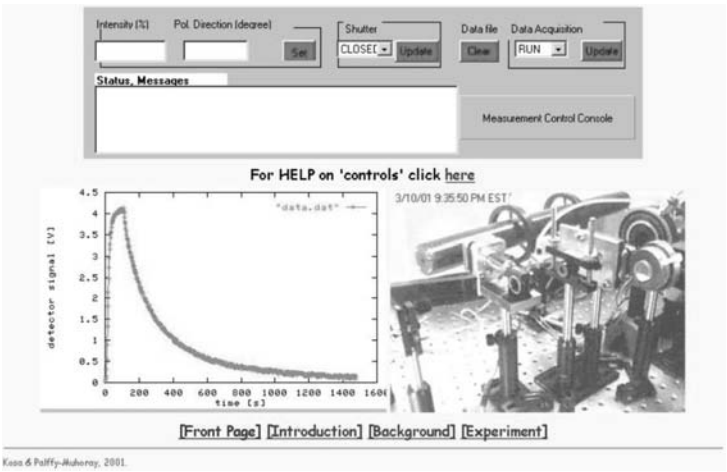

FIGURE 8. Typical frame from the Web-based remote photoinduced twist experiment showing the user interface, detector signal and the experimental setup.

The data shown in Fig. 8 is the intensity at the detector, in response to pump beam turned on at $t = 0$, with polarization parallel to the mechanical buffing direction on the back plate. The pump beam was shut off at $t = 110s$.

EXPERIMENTAL RESULTS & DISCUSSION

Without photoexcitation, the cell adopts the uniform planar state, with the director everywhere parallel to the buffing direction of the mechanically buffed polyimide layer. As the plane polarized pump beam, with polarization parallel to the buffing

direction, is incident on the cell, a twist deformation develops, as indicated by the increased intensity detected by the detector. Typical signals obtained in the experiment are shown in Fig. 9.

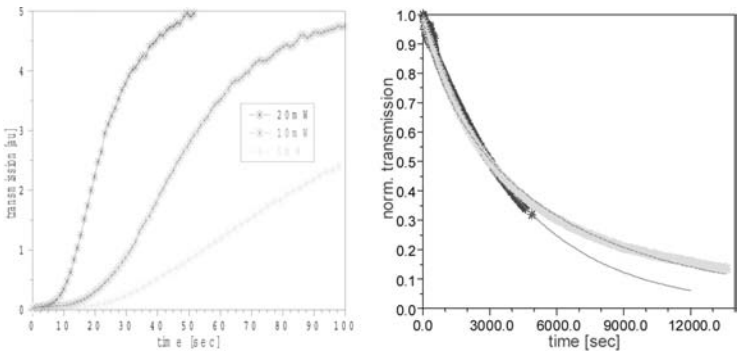

FIGURE 9. Intensity measured at the detector with pump ON and OFF.

Characteristics of the signal are a finite induction time, followed by rapid but pump-intensity dependent increase in the twist which tends to saturate; followed by slow decay of the twist as the pump beam is turned OFF.

First, we note that when the pump beam is turned ON, the direct optical torque $\mathbf{D}\times\mathbf{E}$ on the director is zero; hence the twist cannot be caused by the direct optical torque. Second, we note that the surface torque density acting on the nematic to produce twist through an angle θ_t is $\sim\theta_t K/d$ where K is an elastic constant, and d is the cell thickness. The intrinsic angular momentum current density of the pump is $I\lambda/c$, where I is the intensity, so if torque to cause the twist were to originate from angular momentum transfer from the pump beam, it would require power

$$P=\theta_t w_o^{\,2}\frac{Kc}{\lambda d} \tag{1}$$

where w_o is the beam waist. Estimating $\theta_t=\pi/2$, $w_o=1mm$, $K=10^{-11}N$, we obtain $P\approx 400W$. Experimentally, however, $P=20mW$; it is clear therefore that the torque causing the twist cannot originate in angular momentum transfer from the pump beam. We next turn therefore to a Brownian ratchet description of the dye dynamics.

FOKKER-PLANCK MODEL

We start by considering the interaction energy between the dye molecules and the nematic liquid crystal. For simplicity, we assume that the interaction between the dye molecules in the alignment layer and adjacent liquid crystal molecules can be described by the anisotropic Van der Waals interation, as in Maier-Saupe theory. We assume that we can characterize the orientation of both *trans*- and *cis*- isomers of the dye molecules by a unit vector $\hat{\mathbf{l}}_d$; we take the energy of interaction of the dye molecules in the alignment layer and the adjacent nematic to be

$$U_t = U_{to}(\hat{\mathbf{l}}_d \cdot \hat{\mathbf{n}})^2 \tag{2}$$

for the *trans*- and

$$U_c = U_{co}(\hat{\mathbf{l}}_d \cdot \hat{\mathbf{n}})^2 \tag{3}$$

for the *cis*-isomers; U_{to} and U_{co} are scalar measures of the interaction strengths. We next construct the free energy for the bulk liquid crystal and the photosensitive alignment layer;

$$F = Ad_d \int (\rho_t U_t + kT\rho_t \ln \rho_t + \rho_c U_c + kT\rho_c \ln \rho_c) d^2\hat{\mathbf{l}}_d + \int \frac{1}{2} K((\nabla \cdot \hat{\mathbf{n}})^2 + (\nabla \times \hat{\mathbf{n}})^2) d^3\mathbf{r} \tag{4}$$

here A is the area, d_d is the thickness of the alignment layer, $\rho_t(\hat{\mathbf{l}}_d)$ and $\rho_c(\hat{\mathbf{l}}_d)$ are the number densities of the *trans*- and *cis*-isomers with orientation $\hat{\mathbf{l}}_d$, k is Boltzmann's constant, T is the temperature, K is an elastic constant and $\hat{\mathbf{n}}$ is the nematic director. For simplicity, we have used the one elastic constant approximation. The dynamical equation for the director

$$\gamma \frac{\partial \hat{\mathbf{n}}}{\partial t} = -\frac{\delta F}{\delta \hat{\mathbf{n}}} \tag{5}$$

becomes

$$\gamma \frac{\partial \hat{\mathbf{n}}}{\partial t} = \mathrm{K}(\nabla^2 \hat{\mathbf{n}})(\mathbf{I} - \hat{\mathbf{n}}\hat{\mathbf{n}}) \tag{6}$$

in the bulk, and

$$\gamma_s \frac{\partial \hat{\mathbf{n}}}{\partial t} = \{K(\hat{\mathbf{N}}\nabla\cdot\hat{\mathbf{n}} + \hat{\mathbf{N}}\times\nabla\times\hat{\mathbf{n}}) - d_d\langle\rho_t \frac{\partial U_t}{\partial \hat{\mathbf{n}}}\rangle - d_d\langle\rho_c \frac{\partial U_c}{\partial \hat{\mathbf{n}}}\rangle\}(\hat{\mathbf{d}} - \hat{\mathbf{n}}\hat{\mathbf{n}}) \tag{7}$$

at the surface; γ and γ_s are bulk and surface orientational viscosities; $\hat{\mathbf{N}}$ is the surface normal and the symbol $\langle\rangle$ denotes the average over all orientations. The right hand side of Eq. (7) gives the torques acting on the director at the surface due to elastic distortions in the bulk, and due to surface anchoring due to interactions between the liquid crystal and the dye in the alignment layer. The dynamical equation for the dye *trans*- and *cis*-isomers is obtained from the equation of continuity

$$\frac{\partial \rho}{\partial t} = -\nabla\cdot\mathbf{J} \tag{8}$$

supplemented by creation and annihilation operators. The orientational current is proportional to the chemical potential gradient; that is,

$$\mathbf{J}_t = -M_t\rho_t\hat{\nabla}\mu_t \tag{9}$$

where M_t is the orientational mobility and $\hat{\nabla}$ is the gradient operator on the unit sphere. The chemical potential μ_t of the *trans*-isomer is the derivative of the free energy density with respect to ρ_t; that is,

$$\mu_t = U_t + kT\ln\rho_t \tag{10}$$

to within an additive constant, and the dynamical equation becomes

$$\frac{\partial \rho_t}{\partial t} = D_t\hat{\nabla}^2\rho_t + \hat{\nabla}\cdot(M_t\rho_t\nabla U_t) - \rho_t f_t + \rho_c f_c \tag{11}$$

where the orientational diffusivity $D_t = M_t kT$, and f_t and f_c are transition rates given by

$$f_t = f_{to}e^{U_t/kT} + \nu_t(\hat{\mathbf{l}}_d\cdot\hat{\mathbf{E}})^2 \tag{12}$$

and

$$f_c = f_{co}e^{U_c/kT} + \nu_c(\hat{\mathbf{l}}_d\cdot\hat{\mathbf{E}})^2 \tag{13}$$

The first term in the above expressions consists of the bare transition rates, required to satisfy detailed balance; the second term is associated with photoexcitation. The quantities ν_t and ν_c are the transition rates associated with photoexcitation;

$$\nu_t = \frac{I\sigma_t}{h\nu} \tag{14}$$

I is the pump intensity, $h\nu$ is the photon energy, and σ_t is the absorption cross-section of the *trans-* isomer; the orientation dependence of the absorption is taken into account via the factor $(\hat{\mathbf{l}}_d \cdot \hat{\mathbf{E}})^2$. Similarly, for the *cis-* isomers,

$$\nu_c = \frac{I\sigma_c}{h\nu} \tag{15}$$

It is useful to define the fraction of *trans*-isomers with orientation $\hat{\mathbf{l}}_d$ as

$$\phi_t(\hat{\mathbf{l}}_d) = \rho_t(\hat{\mathbf{l}}_d)/\rho_o \tag{16}$$

and similarly for the fraction of *cis-* isomers

$$\phi_c(\hat{\mathbf{l}}_d) = \rho_c(\hat{\mathbf{l}}_d)/\rho_o \tag{17}$$

where ρ_o is the number density of dye molecules. The dynamics of the system can then be written in dimensionless form as

$$\frac{\partial \phi_t}{\partial \mathrm{t}} = D_t\hat{\nabla}^2\phi_t + \hat{\nabla}\cdot(D_t\phi_t\hat{\nabla}u_t) - \phi_t f_t + \phi_c f_c \tag{18}$$

and

$$\frac{\partial \phi_c}{\partial \mathrm{t}} = D_c\hat{\nabla}^2\phi_c + \hat{\nabla}\cdot(D_c\phi_c\hat{\nabla}u_c) - \phi_c f_c + \phi_t f_t \tag{19}$$

where $u_t = U_t/kT$ and $u_c = U_c/kT$; and

$$\begin{aligned}\frac{\partial \hat{\mathbf{n}}}{\partial t} = \{&D_{LC}d(\hat{\mathbf{N}}\nabla\cdot\hat{\mathbf{n}} + \hat{\mathbf{N}}\times\nabla\times\hat{\mathbf{n}}) \\ &- f_a\langle\phi_t\frac{\partial u_t}{\partial \hat{\mathbf{n}}}\rangle - f_a\langle\phi_c\frac{\partial u_c}{\partial \hat{\mathbf{n}}}\rangle\}(\mathbf{I}-\hat{\mathbf{n}}\hat{\mathbf{n}})\end{aligned} \tag{20}$$

where $D_{LC} = K/(\gamma_s d)$ is the orientational diffusivity of the liquid crystal and $f_a = d_d \rho_o kT/\gamma_s$ is the alignment 'frequency'; the director field in the bulk is obtained from Eq. (6). Eqs. (18),(19) and (20) are the coupled equations which describe the dynamic response of the system.

We have solved these equations numerically using simple discretization and forward time-stepping. Typical results of simulations are shown in Fig. 10.

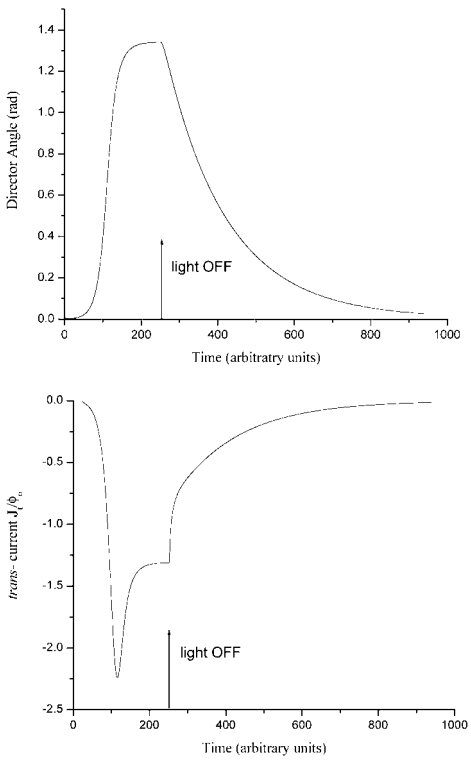

FIGURE 10. Director angle at the photosensitive alignment layer and *trans*-isomer orientational current as function of time.

In the simulation whose results are shown in Fig.10, the following parameters were used: $u_{to} = 0.5$, $u_{co} = 0.0$, $D_t = 1.0$, $D_c = 5.0$, $D_{LC} = 1.0$, $f_{to} = 0.0$, $f_{co} = 5.0$, $\nu_t = 5.0$, $\nu_c = 0.0$ and $f_a = 50.0$. This corresponds to moderately strong interaction between the *trans*- isomer and the nematic field, but no

interaction between the *cis*-isomer and the nematic; an enhanced orientational mobility of the *cis*-isomer relative to the *trans*-, a spontaneous decay of the *cis*-isomer into the *trans*-, and photoexcitation of the *trans*-isomer into the *cis*-form. By tuning these parameters, a relatively broad range of responses can be observed, but these parameters give reasonable qualitative agreement with experiment. Key features are the relatively rapid onset, after a brief induction time, of the twist deformation, resulting from photoexcitation of the dye in the alignment layer, followed by the slow decay of the twist on removing the pump excitation. It is clear from the simulation that the orientational distribution of the dye is strongly altered by the nematic field; in the absence of photoexcitation, the *trans*-isomers tend to align with the director. Photoexcitation results in orientational hole burning, that is, in depopulation of the *trans*- (and population of the cis-) state parallel to the pump polarization, and population of the *trans*- (and depopulation of the cis-) state perpendicular to the pump polarization. As the dye population undergoes this orientational redistribution, the resulting torque on the director causes it to reorient, and twist, near the photosensitive surface, towards the predominant *trans*-isomer orientation perpendicular to the polarization of the incoming pump beam. The effect of the nematic field on the dye distribution plays an important role in determining the dynamic response of the system.

A key feature of the response is that even after equilibrium is reached, while the pump is ON, there exists a steady orientational current of *trans*-isomers as can be seen in Fig. 10. (For the special case considered in this example, only the *trans*-isomer orientational current enters; in a more general case, the *cis*- current could also play a role.) The origins of this current are the same as that of the torque on the director. The average current is given by

$$< \mathbf{J}_t >=< -M_t \rho_t \hat{\nabla} U_t >=< -D_t \rho_o \phi_t \hat{\nabla} u_t > \tag{21}$$

while the anchoring torque acting on the director is

$$\mathbf{O}= -f_a <\phi_t \frac{\partial u_t}{\partial \hat{\mathbf{n}}}> \times \hat{\mathbf{n}} \tag{22}$$

The magnitudes of these are proportional, hence, as expected from Newton's third law, the torque on the director is proportional to the orientational current. We regard therefore the dye molecules in the alignment layers as rotors of Brownian motors, which rotate steadily under photoexcitation in the field of the nematic liquid crystal. This is shown schematically in Fig. 11.

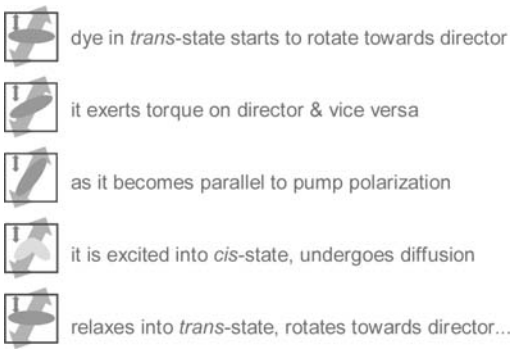

FIGURE 11. Schematic of the Brownian motor scenario.

Once the pump excitation is removed, the orientational distribution of the dye changes again, evolving under the influence of the nematic field. The twist deformation of nematic slowly relaxes; changing the dye distribution in the process. This relaxation is slow, dominated by the coupled evolution of the orientational distribution of the dye and the relaxation of the twist.

SUMMARY

We have considered a photoinduced twist experiment, where light polarized parallel to the director of a planar aligned nematic cell with one photosensitive alignment layer gives rise to a twist distortion. We showed that the twist cannot be the result of angular momentum transfer from light, and argued that the responsible mechanism is an orientational ratchet, where the dye molecules under photoexcitation act as the rotors of Brownian motors in the nematic field. We have pointed out parallels with biological transport. We developed a detailed Fokker-Planck model for the system, and presented the results of simulations; these are in reasonable qualitative agreement with observations. We believe that the only significant difference between the response of our model system consisting of the 'soft' PMMA-DR I alignment layer, which eventually loses the photoinduced orientation of the dye under the influence of the nematic field, and other 'stiff' dyed photoalignment layers[24] is the orientational mobility of the dye molecules in the polymer.

ACKNOWLEDGMENTS

We acknowledge support from the NSF under ALCOM grant 89-DMR20147 and AFOSR MURI grant F49620-17-1-0014.

REFERENCES

[1] A. Ashkin and J.M. Dziedzic, *Phys.Rev. Lett.* **30**, 139 (1973).
[2] R.A. Beth, *Phys. Rev.* **50**, 115, (1936).
[3] A. Saupe, in *Dynamics and Defects in Liquid Crystals*, Ed. P.E. Cladis and P. Palffy-Muhoray (Gordon & Breach, Amsterdam, 1998). The original manuscript was submitted to *Phys. Rev. Lett.* on July 17, (1969).
[4] B.Ya. Zel'dovich, N.F. Pilipetskii, A.V. Sukhov and N.V. Tabiryan, *JETP Lett.* **31**, 264 (1980).
[5] A.S. Zolotko, V.F. Kitaeva,N. Kroo, N.N. Sobolev and L. Csillag, *JETP Lett.* **32**,158 (1980).
[6] I.C. Khoo and S.L. Zhuang, *Appl. Phys. Lett.*, **37**, 3, (1980).
[7] S.D. Durbin, S.M. Arakelian and Y.R. Shen, *Phys. Rev. Lett.* **47,** 1411, (1981).
[8] P. Palffy-Muhoray and W. E, *Mol. Cryst. Liq. Cryst.* **320**, 193, (1998)
[9] I. Janossy, A.DD. Lloyd and B.S. Wherret, *Mol. Cryst.Liq. Cryst.* **179**, 1, (1990).
[10] I. Janossy, *Phys. Rev. E* **49**, 2957, (1994)
[11] L. Marrucci and D. Paparo, *Phys. Rev. E* **56**, 1765, (1977)
[12] R.D. Astumian and M. Bier, *Phys.Rev.Lett.***72**, 1766, (1994).
[13] J. Prost, J.-F. Chauwin, L. Peliti and A. Ajdari, *Phys. Rev. Lett.* **72**, 2652, (1994).
[14] T. Kosa, Weinan E and P. Palffy-Muhoray, *Int. J. Eng. Sci.* **38**, 1077 (2000).
[15] M. Kreuzer, L. Marrucci, D. Paparo, *J. Nonlin. Opt. Phys. & Mats.* **9**, 157 (2000).
[16] C.J. Pennycuick, Newton Rules Biology, (Oxford University Press, Oxford, 1992).
[17] S.M. Block, *Cell,* **87**,151 (1996).
[18] Y. Ishii and T. Yanagida *Single Mol.* **1**, 5 (2000).
[19] Y. Okada and N. Hirokawa, *Science* **283**, 1152 (1999).
[20] R.D. Astumian and I. Derenyi, *Biophys. J.* **77**, 993 (1999).
[21] R.F. Fox and M.-H. Choi, *Phys. Rev. E*, **63**, 1063 (2001).
[22] P. Reimann, "Brownian Motors: noisy transport far from equilibrium" *Physics Reports* (to appear)
[23] R. Landauer, *J. Stat. Phys.* **53**, 233 (1988)
[24] W.M. Gibbons, T. Kosa, P. Palffy-Muhoray, P.J. Shannon and S.T. Sun, *Nature*, **377**, 43 (1995).